Cell

A Role for Neuronal piRNAs in the Epigenetic Control of Memory-Related Synaptic Plasticity

Priyamvada Rajasethupathy,[1] Igor Antonov,[1] Robert Sheridan,[4] Sebastian Frey,[5] Chris Sander,[4] Thomas Tuschl,[5,*] and Eric R. Kandel[1,2,3,*]
[1]Department of Neuroscience
[2]Howard Hughes Medical Institute
[3]Kavli Institute for Brain Sciences
Columbia University, New York, NY 10032, USA
[4]Computational and Systems Biology Center, Memorial Sloan-Kettering Cancer Center, New York, NY 10065, USA
[5]Laboratory of RNA Molecular Biology, Howard Hughes Medical Institute, The Rockefeller University, 1230 York Avenue, New York, NY 10065, USA
*Correspondence: ttuschl@rockefeller.edu (T.T.), erk5@columbia.edu (E.R.K.)
DOI 10.1016/j.cell.2012.02.057

SUMMARY

Small RNA-mediated gene regulation during development causes long-lasting changes in cellular phenotypes. To determine whether small RNAs of the adult brain can regulate memory storage, a process that requires stable and long-lasting changes in the functional state of neurons, we generated small RNA libraries from the *Aplysia* CNS. In these libraries, we discovered an unexpectedly abundant expression of a 28 nucleotide sized class of piRNAs in brain, which had been thought to be germline specific. These piRNAs have unique biogenesis patterns, predominant nuclear localization, and robust sensitivity to serotonin, a modulatory transmitter that is important for memory. We find that the Piwi/piRNA complex facilitates serotonin-dependent methylation of a conserved CpG island in the promoter of CREB2, the major inhibitory constraint of memory in *Aplysia*, leading to enhanced long-term synaptic facilitation. These findings provide a small RNA-mediated gene regulatory mechanism for establishing stable long-term changes in neurons for the persistence of memory.

INTRODUCTION

The lifetime of many human memories runs on the order of years, whereas the RNA or protein molecules that may subserve these memory traces are thought to turn over on the order of days (Price et al., 2010). Several hypotheses have been proposed to explain how memories can remain stable in the face of constant molecular turnover. (1) Prion-like proteins at synapses can adopt active, stable, and self-perpetuating conformations that preclude turnover of the protein (Si et al., 2003, 2010; Bailey et al., 2004). (2) Autoregulatory and positive feedback loops within protein networks can allow persistent enzymatic activity of proteins or newly synthesized protein to take the place of existing protein machinery without loss in state and function (Lisman, 1985; Hayer and Bhalla, 2005; Song et al., 2007; Serrano et al., 2008). (3) And perhaps most tantalizing is the possibility that epigenetic mechanisms such as DNA methylation can alter gene expression and thus the intrinsic properties of neurons in a long-term fashion, perhaps on the order of years (Crick, 1984; Davis and Squire, 1984; Weaver et al., 2004; Miller et al., 2010; Feng et al., 2010).

Small regulatory noncoding RNAs can cause long-lasting changes in cellular phenotypes during development, through their involvement both in autoregulatory feedback loops (Hobert, 2008; Rybak et al., 2008; Krol et al., 2010a) and in the transcriptional and epigenetic regulation of gene expression (Wassenegger, 2005; Saito and Siomi, 2010). To better understand the regulatory roles of miRNAs during long-term memory, we previously generated a miRNA library from the *Aplysia* central nervous system and demonstrated the role of a brain-specific miRNA, aca-miR-124, in constraining long-term synaptic facilitation through repression of the transcriptional activator CREB1 (Rajasethupathy et al., 2009). In the process of mining and characterizing miRNAs from *Aplysia* CNS, we made the unexpected discovery of neuronally expressed piRNAs (Piwi-interacting RNAs).

piRNAs are a class of Piwi-associated, 26–32 nucleotide (nt) small noncoding RNAs (Aravin et al., 2006; Girard et al., 2006; Grivna et al., 2006; Watanabe et al., 2006) that, unlike other small RNAs, are generated from long genomic clusters (Betel et al., 2007) and are thought to have germline-restricted expression. The function of Piwi/piRNA RNP complexes is not fully understood as of yet, but some studies point to a possible role in the epigenetic regulation of transposable elements in the germline through de novo DNA methylation (Aravin et al., 2007; Brennecke et al., 2008; Kuramochi-Miyagawa et al., 2008). Specifically, mice lacking one or more of their Piwi homologs were shown

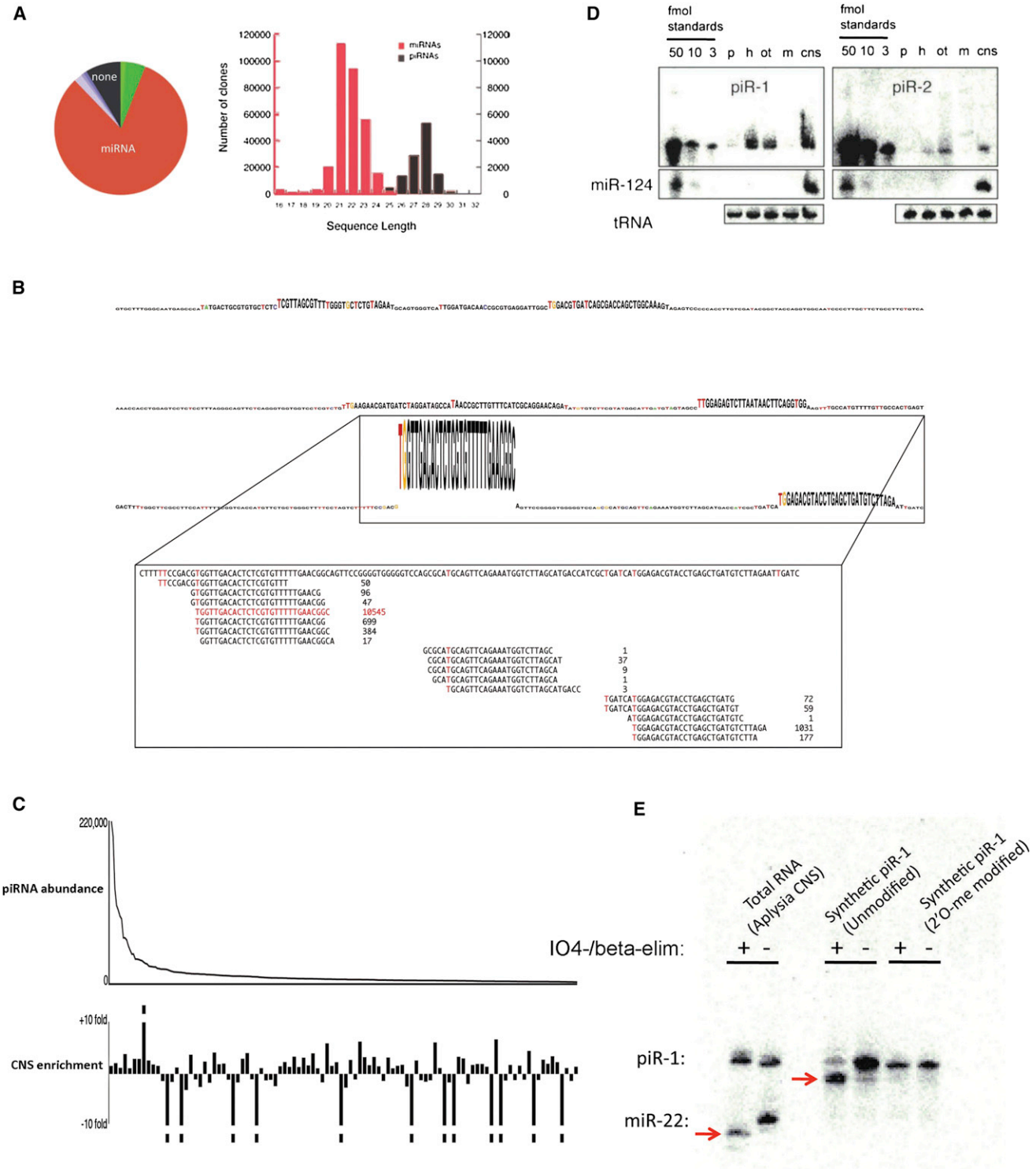

Figure 1. Identification of piRNAs in *Aplysia* Neurons

(A) A size histogram of cloned small RNAs from *Aplysia* CNS revealed two populations, and further characterization confirmed the new class of sequences (shown in black) to be piRNAs.

(B) A continuous genomic region in *Aplysia* encoding a piRNA cluster. A representative 600 bp region within the full 21 kilobase cluster is shown here. The clone frequency of each piRNA is proportional to the height of its nucleotide bases. The clones mapping to the peak piRNA are shown in the inset, and U(T) bias start sites are indicated in red.

(C) The top 100 piRNAs are plotted on the x axis in decreasing order of abundance, and their enrichment in CNS is shown as a positive deflection along the y axis.

to have substantial demethylation and derepression of transposable elements targeted by germline piRNAs.

In a recent study, Lee et al. (2011) reported the identification of piRNAs in mouse neurons. However, comparison of the reported sequences with existing gene annotation suggests that they may instead be fragments of snoRNAs and other abundant RNAs. RNA impurities present in Piwi immunoprecipitates and their subsequent misclassification as piRNAs (Girard et al., 2006) may have contributed to the confusion. Here, we provide a library of bona fide neuronally expressed piRNAs that have been validated in multiple ways: (1) repeated deep sequencing of brain tissue with verification of discovered piRNAs by northerns, (2) confirmation of known properties of piRNAs such as 3′ end modification and stable association with a neuronally expressed Piwi protein, and (3) extensive bioinformatic analysis to show their distinct patterns of clustering within the genome.

We find that *Aplysia* piRNAs are broadly expressed outside of the ovotestes and are amply present in neurons. These piRNAs are abundant, have unique biogenesis patterns, associate with a neuronal Piwi protein, and are distinctly regulated by neuromodulators that are important for learning and memory. By analogy to their role in germline, we find that the Piwi/piRNA complex in neurons can methylate target genes, but in this case, the piRNA we studied targets a critical plasticity-related gene and transcriptional repressor of memory, CREB2 (Bartsch et al., 1995), and methylates its promoter by first accessing its nascent transcript. The DNA methylation of CREB2 by the Piwi/piRNA complex provides a mechanism by which transient external stimuli can cause long-lasting changes in the gene expression of neurons involved in long-term memory storage.

RESULTS

Identification of Neuronal piRNAs in *Aplysia* that Stably Associate with Piwi in Nuclear Compartments

Our previous generation of a small RNA library from *Aplysia* CNS resulted in the majority of sequence reads being mapped as miRNAs, with a minority of reads (~20%) that mapped to the *Aplysia* genome but could not be annotated (Figure 1A). Further examination of these nonannotated small RNA sequences revealed the unexpected presence in brain of another distinct class of small RNAs characterized by a predominant length of 28 nt and a strong preference for a 5′ U (at least 60% of cloned sequence reads for a given piRNA have uridine as the first nucleotide) (Figures 1A and 1B). When these sequences were mapped to the unassembled genome trace files followed by the assembly of larger contigs comprising these regions, we identified clusters containing additional sequences with the same features, revealing a pattern that is characteristic of mammalian piRNAs (see Experimental Procedures for further annotation details). To more comprehensively survey piRNA expression in the *Aplysia* CNS, as well as other tissues, both in the juvenile animal as well as in the adult, we generated anew ten different small RNA cDNA libraries using barcoded adapters and subjected the libraries to deep sequencing using the Illumina platform. Of the sequences that were annotated, the piRNA content per library averaged 15%, compared with the miRNA content, which averaged 60% (Tables S1 and S2 available online). We identified 372 distinct piRNA clusters (Scaffold coordinates provided in Table S2), of which a region of one representative cluster is shown (Figure 1B). *Aplysia* piRNAs exhibit unusual biogenesis patterns in that, within a cluster of piRNA reads, one or a few individual piRNAs were cloned hundreds of times more frequently than surrounding piRNAs in the same cluster (Figure 1B). This piRNA biogenesis pattern leads to an accumulation of specific piRNAs similar in read frequencies to miRNAs (Table S3).

Because piRNAs are preferentially expressed in germline cells in both vertebrates and invertebrates, we anticipated gonad-specific expression in *Aplysia*. Although we find the overall piRNA content (and piRNA-to-miRNA ratio) to be highest in the ovotestes (Table S1), there are several abundant piRNAs that are selectively enriched in the CNS (Figure 1C). To confirm the sequencing data, abundant piRNAs originating from two distinct clusters were analyzed by quantitative northern blots and detected in brain, as well as in ovotestes and heart, but to a lesser extent in other organs such as muscle or hepatopancreas (Figure 1D). Because piRNAs in other species are known to be 2′-O methylated at their 3′ ends, we asked whether neuronal piRNAs in *Aplysia* were also 2′-O methylated at their 3′ ends. We subjected total RNA from *Aplysia* CNS to periodate treatment and beta elimination, followed by northern blot for a piRNA (piR-1) and a miRNA (miR-22). Whereas the miRNA, which was expected to be unmodified at its 3′ end, was sensitive to the treatment and showed an ~2 nt shift (the expected change in mobility upon treatment and elimination of the last nucleotide with a remaining 3′ phosphate), the piRNA did not shift (Figure 2E), suggestive of 2′-O methylation previously documented for piRNAs in other species (Kirino and Mourelatos, 2007).

Consistent with piRNA expression in the CNS, we were also able to clone the full-length cDNA for the 964 aa Piwi protein from the CNS. The sequences of these clones are homologous to vertebrate Piwi proteins and have conserved PAZ and Piwi domains. The *Aplysia* Piwi protein is much more closely related to Piwi proteins by homology than to Argonaute proteins of other species and, within the Piwi family, more closely related to vertebrate than invertebrate Piwi members (Figure 2A), as is often the case with *Aplysia* proteins. We generated a polyclonal antibody for the *Aplysia* Piwi protein that detects the induced recombinant protein, as well as the protein in *Aplysia* neural extracts, as a single band (Figure 2B). To determine whether that the Piwi

(D) Two abundant piRNAs are probed for presence in brain (cns), ovotestes (ot), heart (h), muscle (m), and pancreas (p) by quantitative northern blot. Detection of synthetic piRNAs loaded on the far left of the blots at a concentration of 50, 10, and 3 fmol serve as positive controls and allow quantitation. Blots are reprobed with aca-miR-124 and tRNA to control for specificity of signal and equal loading of samples.

(E) Total RNA extracted from *Aplysia* CNS, either periodate treated with beta elimination (+) or untreated (−), was probed on northern blot for piR-1 and miR-22. piR-1 is insensitive to the treatment and is therefore modified at its 3′ end. miR-22 is sensitive to the treatment (red arrow), shows an ~2 nt shift, and is therefore unmodified at its 3′ end.

See also Tables S1, S2, and S3.

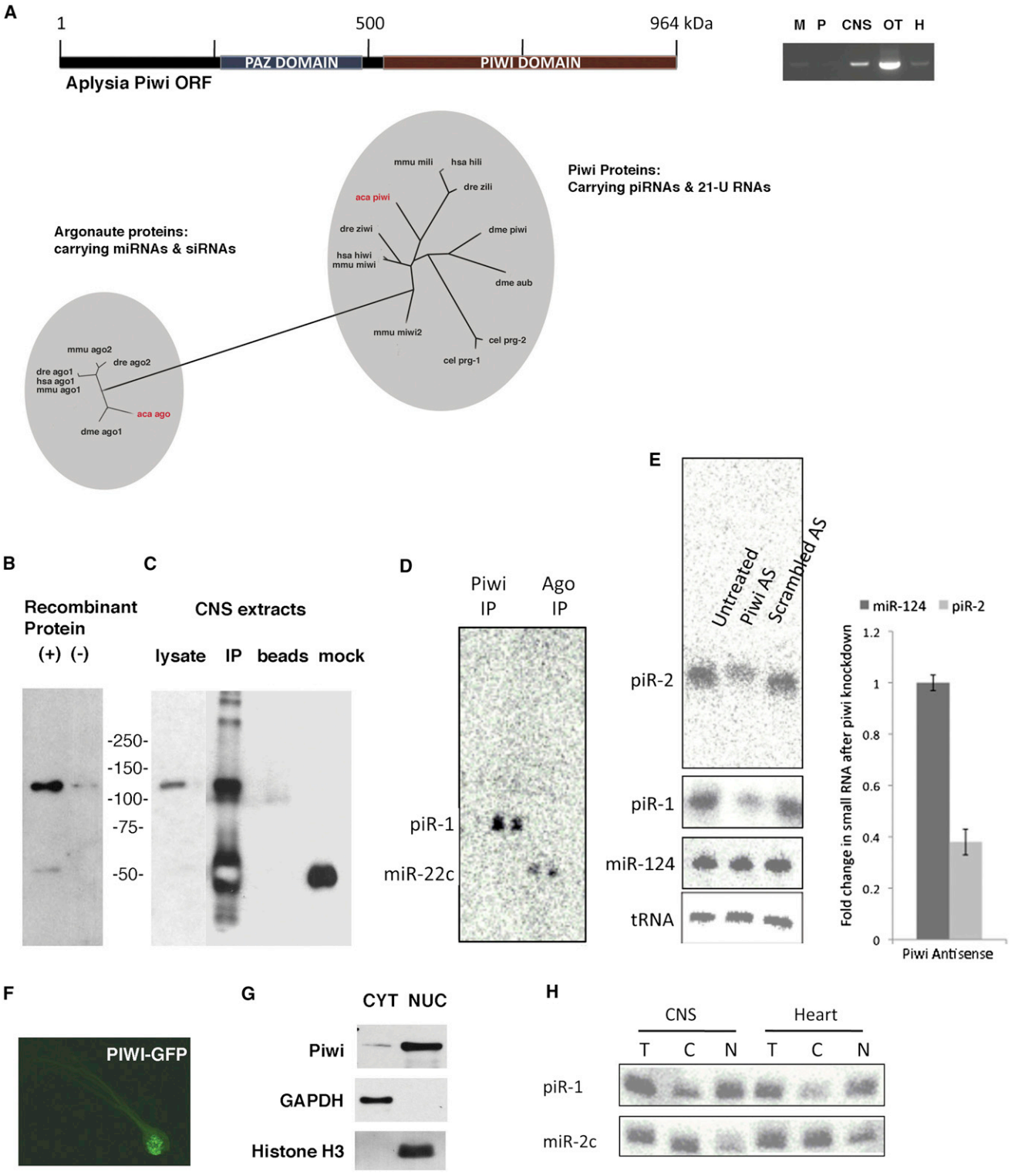

Figure 2. Neuronal piRNAs Stably Associate with a Neuronal Piwi Protein in Nuclear Compartments

(A) The full-length 964 kDa *Aplysia* Piwi protein cloned from *Aplysia* CNS with conserved PAZ and PIWI domains and whose transcript is well expressed in both the ovotestes and CNS. In a homology tree, *Aplysia* Piwi clusters more closely with the Piwi genes of human (hsa), mouse (mmu), zebrafish (dre), fruitfully (dme), and worm (cel) than with the Argonaute genes of those species.

(B) A polyclonal antibody generated against the C-terminal end of the *Aplysia* Piwi protein recognizes induced recombinant Piwi protein at 130 kDa.

protein stably interacts with piRNAs, we immunoprecipitated (IP) Piwi from neural extracts (Figure 2C) and extracted the RNAs from the Piwi complex. When blots of the RNAs from the Piwi IP and Argonaute (Ago) IP were probed for a piRNA (aca-piR-1) and miRNA (aca-miR-22), the piRNA was detected only in Piwi IP, whereas the miRNA was detected only in Ago IP (Figure 2D). We further find that RNA from neural extracts after Piwi knockdown with 2′-O-methyl antisense oligoribonucleotides (Piwi knockdown confirmed in Figure 4A) are depleted in piRNAs when compared to control extracts, with no detectable change in the levels of other noncoding RNAs, such as miRNAs or tRNA (Figure 2E). These experiments demonstrate that there are indeed two distinct classes of small RNAs in *Aplysia* CNS, miRNAs, and piRNAs, each of which associates with its respective Ago and Piwi protein.

To better understand the subcellular localization of Piwi and piRNAs in *Aplysia* neurons, we first separated neural protein and RNA extracts into nuclear and cytoplasmic fractions and probed for the Piwi protein on western blots and piRNAs on northern blots. Effective fractionation was confirmed by the presence of GAPDH only in cytoplasmic compartments and histone H3 in nuclear compartments. We detected the Piwi protein primarily in the nuclear compartment (Figure 2G). Consistent with this finding, overexpression of GFP-tagged Piwi in *Aplysia* sensory neurons shows a predominant nuclear localization of the Piwi protein (Figure 2F). A northern blot comparing small RNA content in the nuclear and cytoplasmic fractions with total unfractioned RNA also revealed that the piRNAs were primarily nuclear, whereas the miRNAs were primarily cytoplasmic (Figure 2H). Taken together, both Piwi and piRNAs in *Aplysia* neurons have predominant nuclear localization, suggesting a nuclear function for the Piwi/piRNA complex.

Piwi/piRNA Complexes Enhance Memory-Related Synaptic Plasticity by Regulating the Transcriptional Repressor CREB2

To determine whether piRNAs have a regulatory role in memory-related synaptic plasticity, we screened some of the abundant neuronal piRNAs for changes in expression levels upon exposure to serotonin (5HT), a neuromodulator that is important for learning and memory. A subset of the selected piRNAs was significantly upregulated (Figure 3A). aca-piR-4 and aca-piR-15 are examples of piRNAs that were robustly induced by 5HT. The former was transiently induced, whereas the latter had a more delayed but enduring activation. The increase in piRNA expression in response to 5HT was particularly interesting in comparison with the activity of several *Aplysia* miRNAs, which by contrast, were rapidly downregulated in neurons in response to neuromodulators and to neuronal activity (Rajasethupathy et al., 2009). These observations suggest that the two classes of small RNAs in the *Aplysia* CNS could exercise coordinated bidirectional activity of their targets during memory-related synaptic plasticity.

To better understand the functional relevance of these 5HT-induced piRNAs, we explored their role in memory-related synaptic plasticity in cultured neurons in response to 5HT. The cocultures used in these experiments consisted of two sensory neurons that each synapse on a single target motor neuron. We first depleted Piwi (and consequently its associated piRNA population) from sensory neurons that form synapses with motor neurons in culture and assayed for changes in the strength of the sensory-motor synapse. We injected an antisense 2′-O-methyl oligoribonucleotide to Piwi in one sensory neuron of the coculture, and the other sensory neuron was left unmodified as an internal control. In each case, electrical activity was recorded in the motor neuron after exposure to 5HT to determine the change in baseline synaptic transmission and in memory-related long-term facilitation (LTF) at these synapses. We found that knockdown of Piwi significantly impaired LTF as measured at 24 and 48 hr after exposure to five pulses of 5HT ($n = 34$), when compared with uninjected controls in the same coculture ($n = 37$; $F_{(3,95)} = 13.63$; $p < 0.001$ repeated measures ANOVA; $p < 0.02$ and $p < 0.04$ at 24 and 48 hr, respectively, Newman-Keuls post hoc test; Figure 3C). The observed differences between the two groups were not due to differences in the basal strength of the synaptic connections. We confirmed the efficacy of Piwi knockdown by western blotting, as the antibody was not able to detect Piwi by immunostain (Figure 4A), and we also confirmed that the Piwi knockdown specifically prevented the accumulation of mature piRNAs (Figure 2E). Control experiments with the injection of scrambled antisense 2′-O-methyl oligoribonucleotides did not show changes in LTF ($n = 23$, scrambled AS versus $n = 9$, 5 × 5-HT; $p > 0.6$ at both 24 and 48 hr, Newman-Keuls post hoc test; Figure 3D). We next determined whether overexpression of Piwi had the opposite effect. Overexpression of Piwi-GFP ($n = 22$) caused a significant enhancement of 5HT-dependent long-term synaptic facilitation with respect to untreated controls ($n = 40$) as measured at 24 and 48 hr ($F_{(2,78)} = 44.04$; $p < 0.001$ repeated measures ANOVA; $p < 0.001$ Newman-Keuls post hoc test at both 24 and 48 hr; Figure 3E). Taken together, we conclude that 5HT induces the activity of Piwi-associated piRNAs, which in turn act to enhance LTF.

To identify genes through which Piwi might act to enhance 5HT-dependent long-term facilitation, we screened many

(C) The antibody also recognizes Piwi protein from *Aplysia* neural extracts and is able to specifically IP the protein as a single band at 130 kDa.
(D) RNA from Piwi IP and Ago IP were northern blotted and probed for a piRNA (aca-piR-1) and a miRNA (aca-miR-22). The piRNA is only detected in the Piwi IP, whereas the miRNA is only detected in the Argonaute IP.
(E) The Piwi knockdown samples had a specific depletion in piRNAs (aca-piR-1 and aca-piR-2) but no change in miRNA or tRNA levels, confirming that knockdown of Piwi specifically prevents maturation of piRNAs. Changes in piRNA levels are quantified and are presented as a mean of three independent trials ± SD.
(F) Overexpression of *Aplysia* Piwi protein with GFP tagged at the C terminus reveals a nuclear localization of Piwi in sensory neurons.
(G) Nuclear (NUC)/cytoplasmic (CYT) fractionation of neuronal proteins followed by western blot revealed a nuclear localization for Piwi protein. GAPDH is detected only in the cytoplasmic fraction, and histone H3 is detected only in the nuclear fraction, confirming effective fractionation.
(H) Nuclear (N)/cytoplasmic (C) fractionation of total (T) RNA followed by northern blot revealed a nuclear enrichment of piRNA and cytoplasmic enrichment of miRNA.

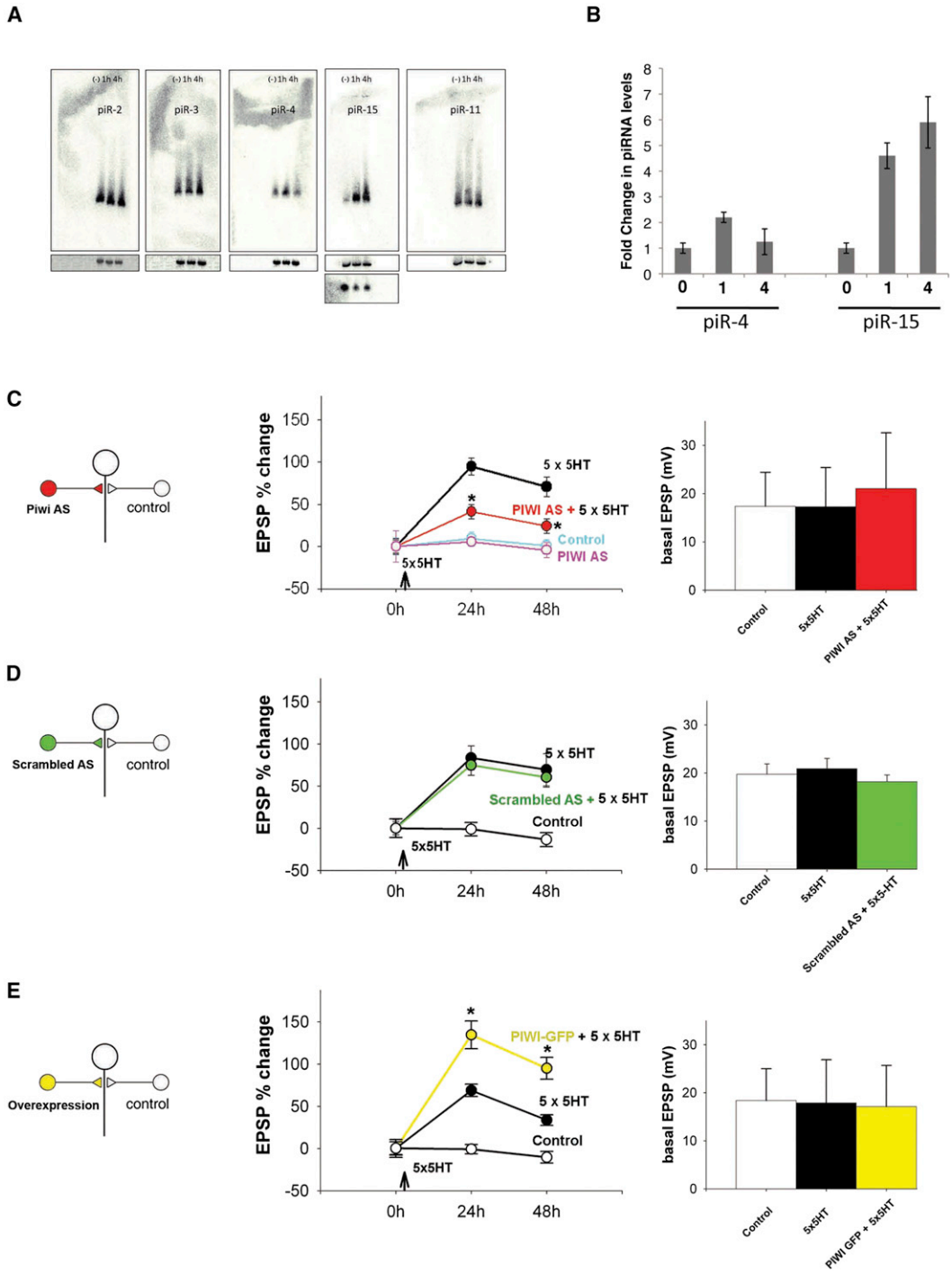

Figure 3. Piwi/piRNAs Enhance Serotonin-Dependent Memory-Related Synaptic Plasticity

(A and B) *Aplysia* CNS were treated either with vehicle (−) or with 5 × 5HT, and RNA was extracted 1 hr and 4 hr later and northern blotted. tRNA bands are shown to control for equal loading of samples. Changes in piRNA levels are quantified in (B) and are presented as a mean of four independent trials ± SD.

(C–E) Graphs reporting the percentage change in the excitatory postsynaptic potential (EPSP) amplitude measured at 24 hr and 48 hr after 5 × 5HT application with respect to pretreatment values in the different experimental groups. In each coculture, one of the two sensory neurons was injected with 5 M Piwi antisense (C), scrambled negative control (D), or Piwi-GFP (E), whereas the other sensory neuron was left untreated as a control. Changes in EPSP levels are quantified in and presented as a mean of 37 (C), 23 (D), and 22 (E) independent trials ± SD. The observed differences between treatment groups are not due to differences in basal synaptic strength.

plasticity-related genes for changes in expression levels after knockdown of Piwi. Desheathed pleural ganglia were incubated in antisense 2′-O-methyl oligoribonucleotides conjugated with penetratin to inhibit Piwi (confirmed by western blot; Figure 4A), and total protein was extracted and western blots prepared and probed with specific antibodies. We found that inhibition of Piwi led to a reproducible 2-fold upregulation of the transcriptional repressor and major inhibitory constraint on LTF, CREB2, when compared to neurons treated with scrambled control 2′O-methyl oligoribonucleotides. This effect was specific to CREB2, as Piwi inhibition had no effect on several other plasticity-related genes such as C/EBP and CPEB (Figure 4A). The observed increase in CREB2 protein levels was supported by an even greater increase in CREB2 mRNA levels (Figure 4B).

In earlier studies, it was observed that knockdown of CREB2 in sensory neurons could prime the sensory-motor synapse such that a weak stimulus (one pulse instead of five pulses of 5HT) was sufficient to cause LTF that lasts days (Bartsch et al., 1995). We therefore asked whether overexpression of Piwi, through its repression of CREB2, could prime neurons in a similar way. Indeed, we found that cells overexpressing Piwi (n = 15) gave rise to LTF when exposed to just a single pulse of 5HT, whereas control cells (n = 25) required five pulses of 5HT to elicit LTF that could last days ($F_{(4,100)} = 5.05$; $p < 0.001$ repeated measures ANOVA; $p < 0.001$ Newman-Keuls post hoc test at 24 and 48 hr; Figure 4C). The facilitation produced by one pulse of 5HT was robust, as it was observed in 13 out of 15 Piwi-overexpressing cells. Moreover, the facilitation seen at 24 hr with one pulse was comparable in magnitude to that seen at 24 hr in control cells treated with five pulses of 5HT. In earlier studies (Bartsch et al., 1995), though knockdown of CREB2 allowed for priming by 1 pulse of 5HT, there was no enhancement of LTF seen from five pulses of 5HT. Our observation, therefore, that Piwi-overexpressing cells enhance LTF from five pulses of 5HT (Figure 3E), suggests that Piwi likely has other targets in addition to CREB2. In summary, the sensitivity of Piwi-overexpressing cells to one pulse of 5HT suggests that it primes neuronal activity through regulation of CREB2, whereas the enhancement of LTF caused by five pulses in Piwi- overexpressing cells suggests that Piwi likely regulates other genes as well, in addition to CREB2.

CREB2 Is Methylated at Its Promoter in Response to 5HT-Induced Synaptic Plasticity

To gain insight into the mechanism of CREB2 regulation by Piwi, we asked whether 5HT acts on CREB2 at the level of transcription, as suggested by the nuclear localization of Piwi and its effect on both CREB2 protein and RNA levels. Earlier studies followed CREB2 expression levels up to 3–4 hr after exposure to 5HT, and in this time frame, no change in CREB2 protein or RNA was noted (Bartsch et al., 1995). We therefore monitored the levels of CREB2 for days after the initial exposure to 5HT and noticed that CREB2 protein levels begin to drop at 12 hr and continue to remain low for up to 48 hr without returning to the initial baseline level of expression (Figure 4D). This long-lasting drop in CREB2 levels is consistent with and may be responsible for the observation that 5HT induces long-lasting elevation in the transcriptional activator CREB1 (Liu et al., 2008). At the protein level, the reduction in CREB2 levels was modest, but the effect was more pronounced at the mRNA level (Figure 4E). The long-lasting effect on both the CREB2 protein and RNA levels suggests that a stable 5HT-dependent repressive state is established. Because Piwi and piRNAs have known roles in epigenetic regulation in the germline through DNA methylation, we asked whether CREB2 also is being regulated by Piwi through methylation at its promoter.

The *Aplysia* DNA methyltransferase (DNMT) is well expressed in neurons (Moroz et al., 2006), and its enzymatically active domain is highly conserved among the vertebrate homologs of DNMTs. We therefore inhibited ApDNMT enzymatic activity chronically in neurons with the DNMT inhibitor RG108 and observed a strong increase in CREB2 levels. To determine whether DNMT activity on CREB2 was dependent on 5HT, we applied RG108 to neurons in the presence of 5HT and found that, 12 hr later, the 5HT-dependent long-lasting downregulation of CREB2 was abolished (Figure 4F). These effects of RG108 appear to be specific to CREB2, as there was no significant upregulation of CREB1 levels. In fact, a modest downregulation was apparent. To determine whether the effects of DNMT inhibition on CREB2 levels were functionally important during memory-related plasticity, we again performed electrophysiological experiments on sensory-motor cocultures in the absence and presence of RG108. Remarkably, bath application of the inhibitor RG108 (n = 38) almost fully abolished 5HT-dependent long-term facilitation with respect to controls (n = 37), as measured at both 24 and 48 hr ($F_{(3,100)} = 12.86$; $p < 0.001$ repeated measures ANOVA; $p < 0.03$ and $p < 0.02$ at 24 and 48 hr, respectively, Newman-Keuls post hoc test; Figure 4G). The effect of RG108 was entirely dependent on 5HT, as the application of RG108 alone in the absence of 5HT had no effect on the baseline activity of the cells (Figure 4G).

To determine whether DNMT acted indirectly on CREB2 or whether it directly methylated the promoter of CREB2, we examined its promoter region for possible CpG islands. We found two predicted CpG islands, one that is proximal to the translational start site (~200 bp upstream of the first ATG) and that encompasses a CRE-binding element and TATA-binding site and the other that is distal (~700 bp upstream of the first ATG) (Figure 5A). We also noticed that the promoter of ATF4, the human homolog of CREB2, contains a conserved CpG island (http://genome.ucsc.edu). To test whether either of the predicted CpG islands was functional, we extracted genomic DNA and treated it with bisulfite. This procedure allows recognition of methylated bases in DNA (Callinan and Feinberg, 2006) because bisulfite converts all genomic cytosine residues to uridine excepting the methylated cytosines, which are inert to bisulfite treatment. By scoring the C-to-T conversion rates of the CpG sites in genomic DNA after bisulfite treatment, one can determine the fraction of DNA at every CpG site that exists in the methylated versus unmethylated state. We first asked whether methylation-specific primers (MSP; designed to detect only the methylated copies of genomic CREB2) have a differential ability to amplify genomic DNA from cells that either have or have not been treated with 5HT. We found that exposure to 5HT dramatically increases the methylated fraction of the proximal CpG island, but not the distal CpG island (Figure 5A). We next designed both USPs

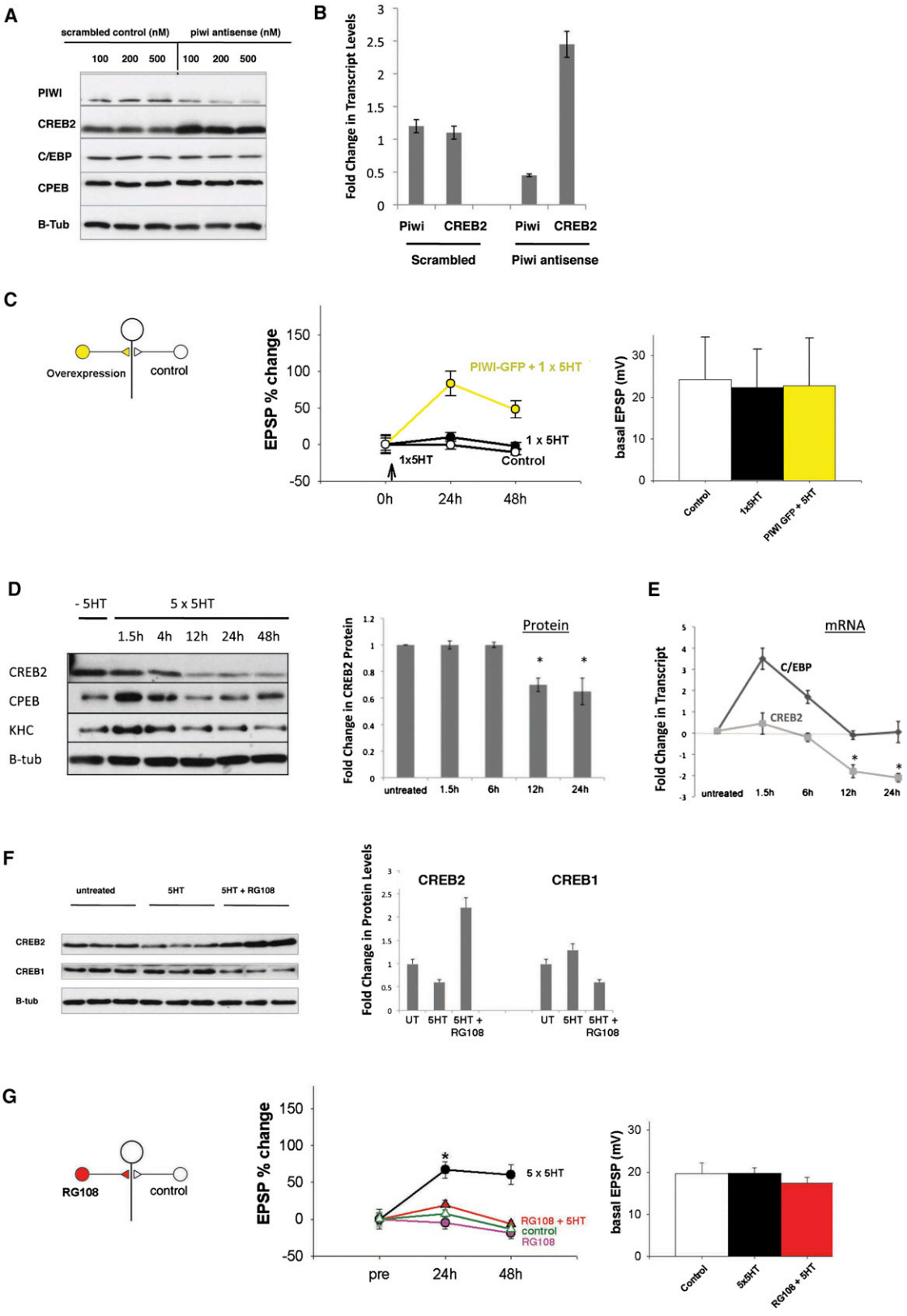
A
scrambled control (nM)
piwi antisense (nM)
100 200 500 100 200 500
PIWI
CREB2
C/EBP
CPEB
B-Tub
B
Fold Change in Transcript Levels
Piwi CREB2 Piwi CREB2
Scrambled
Piwi antisense
C
Overexpression
control
EPSP % change
PIWI-GFP + 1 x 5HT
1 x 5HT
1x5HT
Control
0h 24h 48h
basal EPSP (mV)
Control
1x5HT
PIWI GFP + 5HT
D
- 5HT
5 x 5HT
1.5h 4h 12h 24h 48h
CREB2
CPEB
KHC
B-tub
Protein
Fold Change in CREB2 Protein
untreated 1.5h 6h 12h 24h
E
mRNA
C/EBP
CREB2
Fold Change in Transcript
untreated 1.5h 6h 12h 24h
F
untreated
5HT
5HT + RG108
CREB2
CREB1
B-tub
CREB2
CREB1
Fold Change in Protein Levels
UT 5HT 5HT + RG108
UT 5HT 5HT + RG108
G
RG108
control
EPSP % change
5 x 5HT
RG108 + 5HT
control
RG108
pre 24h 48h
basal EPSP (mV)
Control
5x5HT
RG108 + 5HT

(unmethylated-specific primers, designed to detect only the unmethylated copies of genomic DNA) and MSPs for the promoter regions of CREB2 and CREB1 to compare the fractional representation of the methylated and unmethylated states of the CpG islands at baseline and after exposure to 5HT. We found that, in the basal state, the CREB2 promoter exists in both methylated and unmethylated forms, but 12 hr after exposure to 5HT, the promoter is almost entirely in the methylated form, and in the presence of DNMT inhibitors, the promoter is almost entirely in the unmethylated form (Figure 5B). This pattern of methylation of the CREB2 promoter is in direct contrast to the CREB1 promoter, which exists almost entirely in the unmethylated form at baseline, remains unmethylated after exposure to 5HT, and again remains unmethylated in the presence of DNMT inhibitors (Figure 5B).

To more quantitatively measure the methylated and unmethylated fraction of the CREB2 promoter, we designed primers that lie outside of the proximal CpG island and amplified the region in between by pyrosequencing to score the C-to-T conversions at every CpG site. Because the C-to-T conversion rate at each site reflects the unmethylated fraction, to display percent methylation, we plot 1 – (C to T conversion rate) at each CpG site. We found that, at baseline, almost every CpG site in the CREB2 promoter exists in ~50% methylated form, which is striking particularly when compared with the promoters of CREB1 and PKA-R, which display little to no methylation (Figures 5C, 5D, and 5E). This finding suggests that the CREB2 promoter is dynamically regulated by methylation and that its methylation state at baseline may reflect experience. After exposure to 5HT, every CpG site within the CpG island of CREB2 has increased methylation, with those at the beginning and end of the CpG island showing the most significant increase (Figure 5C). Extraction and bisulfite treatment of genomic DNA after exposure to DNMT inhibitors prevents, as expected, the 5HT-induced increase in methylation and drops methylation levels to below baseline (Figure 5C). Taken together, these data reveal that 5HT causes direct methylation of the proximal CpG islands in the CREB2 promoter and that this methylation leads to a long-term downregulation of CREB2 RNA and protein levels, which may be responsible for the resulting persistence of memory-related synaptic plasticity.

Piwi/piRNA Complexes Control the Methylation State of the CREB2 Promoter

Given that Piwi is regulating CREB2 at the transcriptional level (Figures 4A and 4B), we asked whether Piwi was required for the observed serotonin-dependent methylation of CREB2 in neurons. We inhibited Piwi in sensory neurons and extracted the genomic DNA after exposure to 5HT. Following bisulfite treatment, we scored the percent methylation by pyrosequencing and found that inhibition of Piwi completely abolished the serotonin-dependent increase in methylation at the promoter (Figure 6A). The reversal in methylation patterns was most significant at the beginning and ends of the CpG island, consistent with the observation that the same sequence areas were most sensitive to serotonin (Figure 6A). To determine which piRNA mediates this effect, we searched the CREB2 locus for potential piRNA-bindings sites and identified four well-expressed candidate piRNAs that had good complimentary to the promoter, 5′ UTR, and initial coding segment of the CREB2 mRNA (Figure 6B). Through a series of knockdown experiments using 2′-O-methyl oligoribonucleotides specific to each of the four piRNAs, we observed that one piRNA, aca-piR-F, had the strongest effect on CREB2 expression. Knockdown of aca-piR-F, but not aca-piR-A, C, or D, increased the baseline levels of CREB2 both at the protein and RNA level, demonstrating that aca-piR-F is a transcriptional regulator of CREB2 (Figure 6C). The effects of piR-F are specific because use of 4 nt mismatch oligos antisense to piR-F had no effect on CREB2 levels (Figure 6C). If aca-piR-F were indeed mediating the observed 5HT-dependent methylation effects of CREB2, then aca-piR-F should be regulated by 5HT on a similar time course. We followed aca-piR-F levels with exposure to 5HT as a function of time and noticed a slightly delayed but more enduring upregulation of aca-piR-F that peaked at 3–4 hr before dropping back to baseline at 12 hr (Figure 6D). This time course is consistent with the observed drop in CREB2 RNA levels, which begin at 6 hr after exposure to 5HT. Because the putative binding site for aca-piR-F lies near the translational start site of CREB2, we propose a model in which the Piwi/piRNA complex, through aca-piR-F, binds the nascent CREB2 transcript, thereby bringing it within close proximity for regulation of the CREB2 promoter during 5HT-dependent

Figure 4. Piwi Transcriptionally Regulates CREB2 in a Serotonin- and DNMT-Dependent Manner

(A) Knockdown of Piwi causes a robust upregulation of CREB2, which is specific, as there is no significant change in expression levels of C/EBP or CPEB.

(B) Real-time PCR experiments show that knockdown of Piwi produces a significant increase in CREB2 RNA levels when normalized to GAPDH levels (effects quantified as a mean of four independent trials ± SD).

(C) Electrophysiology experiment reporting percentage change in EPSP amplitude measured at 24 hr and 48 hr after 1 × 5HT with respect to pretreatment values for neurons overexpressing Piwi-GFP, as compared to control cells. The effects observed were quantified as a mean of 15 independent trials ± SD and were not due to changes in the baseline strength of Piwi-GFP versus control synapses.

(D) *Aplysia* sensory neurons were either treated with vehicle or 5HT, and protein was subsequently extracted at 1.5, 4, 12, 24, and 48 hr after 5HT. CREB2, CPEB, and KHC levels were monitored. Blots were reprobed for tubulin to control for equal loading of samples. This exact time course was run only once, but a similar time course is shown quantified in the next panel as a mean of three independent trials ± SD.

(E) Real-time PCR experiments showing that CREB2 RNA levels have a long-lasting and more robust downregulation after exposure to 5HT. The 5HT-dependent early induction of C/EBP mRNA (a known immediate early gene) from the same preparation is shown as a positive control. The change in RNA levels are shown as a mean of six independent trials ± SD.

(F) Three independent experiments each of neurons treated with vehicle, 5HT, or 5HT in the presence of a DNA methyltransferase inhibitor (RG108) are shown where the proteins were extracted 12 hr later and western blotted. CREB2 is downregulated by 5HT, and this effect is reversed in the presence of RG108. The opposite is observed for CREB1. The results are quantified as a mean of three independent trials ± SD.

(G) Electrophysiology experiment reporting percentage change in EPSP amplitude measured at 24 hr and 48 hr after 5 × 5HT with respect to pretreatment values for neurons treated with RG108, as compared to control population. The change in EPSP was quantified as a mean of 38 independent trials ± SD. The inhibitor was confirmed to not be toxic to the cells, as application of the inhibitor alone in the absence of 5HT had no effect on the baseline strength of the synapses.

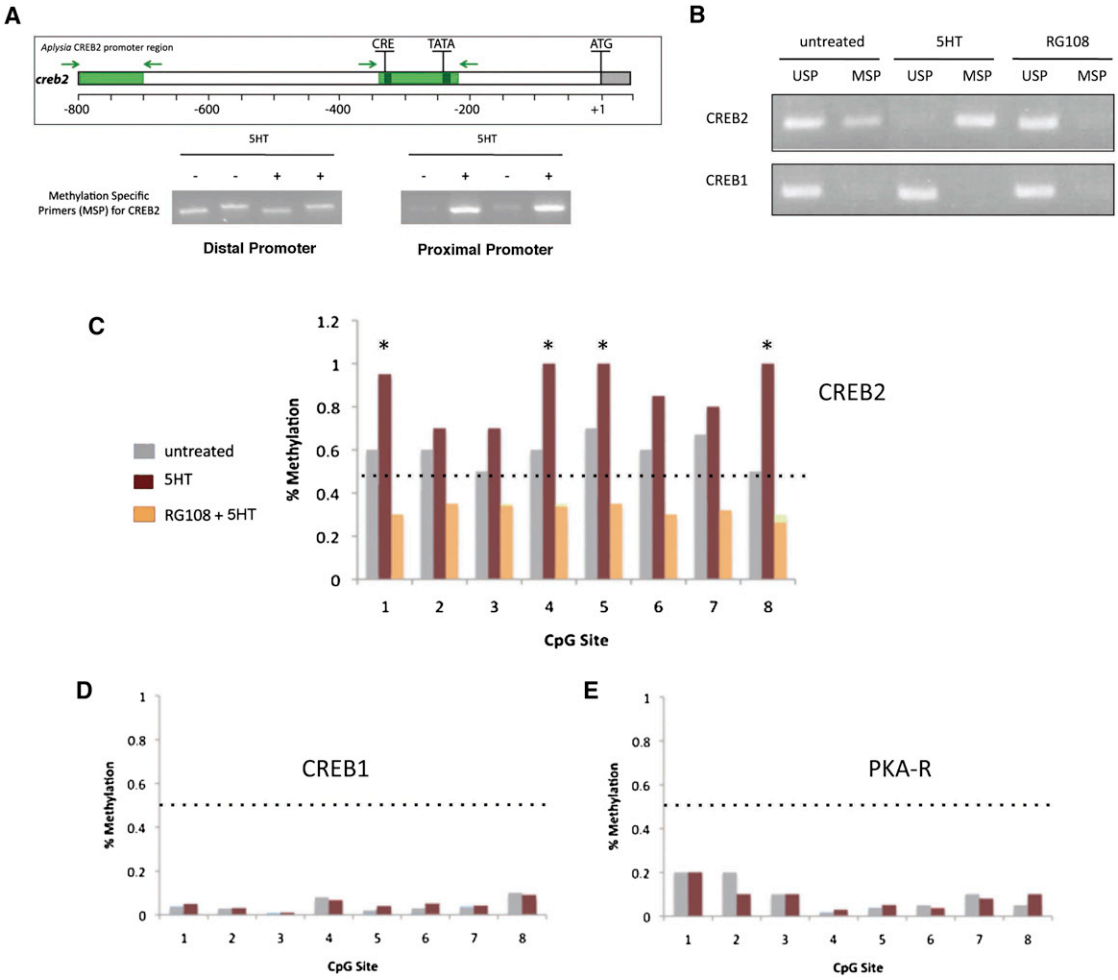

Figure 5. Serotonin Induces Methylation at the CREB2 Promoter

(A) The genomic locus for *Aplysia* CREB2 is shown, and areas in green are predicted CpG islands. Methylation-specific primers (MSP) designed to detect methylation at the distal CpG island show no change in methylation patterns within 12 hr after exposure to 5HT. MSPs designed for the proximal CpG island detect higher levels of methylation in 5HT-treated samples (+) compared with controls (−).

(B) Using MSPs and USPs (unmethylation-specific primers), we detected the ratio of the methylated to the unmethylated form of the CREB2 promoter under baseline conditions and compared with 5HT and RG108 treated samples. CREB2 promoter shifts entirely to the methylated form with exposure to 5HT and back to the unmethylated form with DNMT inhibitor RG108. CREB1 always exists in the unmethylated form.

(C–E) Real-time pyrosequencing of the CREB2 promoter region shows a significant baseline level of methylation (gray) at individual CpG sites that is robustly upregulated with exposure to 5HT (maroon), and this effect is abolished in the presence of the DNMT inhibitor RG108 (orange). Effects were quantified as the mean of four independent trials, and SDs were calculated but so low that they are not shown on the graphs for clarity of the figure. These effects are specific to CREB2, as neither CREB1 (D) nor PKA-R (E) promoters show significant baseline methylation or any serotonin-dependent changes in methylation status.

long-term memory (Figure 6E). The observed stable silencing of CREB2 by the Piwi/piRNA complex (Figure 6), when placed in the context of Figures 4A and 4B in which transient knockdown of Piwi reverses CREB2 silencing, is suggestive of active demethylation at the CREB2 promoter. Though this is consistent with a wider literature that demonstrates active and ongoing demethylation of promoters in adult neurons, we in this study have not explicitly demonstrated active demethylation of the CREB2 promoter. Transcriptional control of gene expression through complementary base-pairing of a small RNA with a nascent mRNA transcript has been previously discovered, first in the exciting work from *S. pombe* and more recently from a study in *C. elegans* (Verdel et al., 2004; Guang et al., 2010).

DISCUSSION

The discovery that piRNAs exist outside the germline in several major organs of *Aplysia*, but significantly in the nervous system, suggests much broader roles for piRNAs than have been previously appreciated. In addition to their presence and in certain cases enrichment in neurons, *Aplysia* piRNAs are unique from those previously described in that they derive from hot spots in

the genome where they are abundantly expressed, and notably, several piRNAs are regulated by neuromodulators that are important for learning-related synaptic plasticity, suggesting functions in memory storage.

An understanding of the role of piRNAs in the epigenetic regulation of long-term memory is significant for several reasons. First, the role of epigenetic modifications in differentiated cells, especially in adult neurons, has been controversial. It is commonly thought that changes in gene expression during development are permanent but that they are not permanent in adult neurons, where the plastic nature of synaptic connections by definition requires bidirection and reversible changes in gene expression. In recent years, the identification of DNA demethylase activity in adult neurons (Barreto et al., 2007; Rai et al., 2008; Ma et al., 2009) brought forth the possibility that epigenetic changes in the adult brain may not necessarily be permanent but may simply be more long-lasting and more permanent than the other known modifications so far described. Subsequent studies have identified individual gene loci that are methylated in response to neurotransmitter activity, though the time course of onset and persistence of methylation are unclear and require further study. Our study provides a piRNA-mediated mechanism for epigenetic regulation in neurons and, further, explores the electrophysiological properties of DNA methyltransferase and of Piwi in synaptic plasticity.

The finding that the Piwi/piRNA complex regulates the CREB2 promoter by DNA methylation in an activity-dependent manner provides an attractive explanation for how neurons translate transient stimuli into stable internal representations and is consistent with several earlier studies that show a role for epigenetic regulation in memory (Guan et al., 2002; Miller et al., 2010; Feng et al., 2010). Our data on the variability in baseline CREB2 methylation levels suggest further that each neuron may have a different basal level of CREB2 expression, which reflects its experience and immediate history. This would be consistent with earlier observations showing that variations in baseline levels of CREB1 across populations of neurons in the amygdala determine the sequence in which these neurons are recruited for memory and for recall (Han et al., 2007). Because CREB2 is antagonistic to CREB1, long-lasting changes in CREB2 levels could set up this CREB1 distribution in neuronal cells, based on experience, which in turn could dictate which neurons are already holding a memory trace and which neurons are readily drawn into new memory traces (Han et al., 2007; Won and Silva, 2008).

The discussion above, however, does not address the question of how Piwi-mediated transcriptional and therefore cell-wide changes in neuronal excitability (intrinsic plasticity) effectively mediate synapse-specific events (synaptic plasticity)? As studies previously have emphasized, it is likely that both forms of plasticity coexist such that one can fine-tune the other, but it is also possible that, in certain contexts, the two exist entirely independently. Though synaptic plasticity affords orders of magnitude more computational power and is therefore ideal for storage of explicit memories requiring attention to detail, intrinsic plasticity, such as those driven by piRNA-mediated epigenetics, has the advantage of priming memories and allowing for robust generalized learning, wherein the same association rules are applicable to experiential learning in various contexts. Because human life is characterized by a great deal of habit formation and repetition-based associative learning, the use of intrinsic plasticity alone in some parts of the human brain may turn out to be an efficient method for this type of memory storage.

Future work on the role of small RNAs in learning and memory should provide further insight into the varying roles of miRNAs versus piRNAs. Though notable exceptions exist (Wayman et al., 2008; Fiore et al., 2009), we and others have previously found a rapid turnover of several neuronal miRNAs in response to neuromodulators and neuronal activity (Rajasethupathy et al., 2009; Krol et al., 2010b), which contrasts to the slow but more enduring upregulation of the few neuronal piRNAs observed in this study. In addition, whereas aca-miR-124 (Rajasethupathy et al., 2009) and another brain-specific miRNA (F. Fiumara, P.R., T.T., and E.R.K., unpublished data) constrain serotonin-dependent long-term facilitation, Piwi-dependent piR-F enhances it. We currently have very few cases from which to draw generalizable conclusions, but future large-scale studies of small RNA function in neurons may highlight the possible existence of two distinct classes of small RNAs that are bidirectionally regulated by neuromodulators and that act on a functionally segregated population of targets to effect either facilitation or constraint on memory-related synaptic plasticity. Further studies would also benefit from genome-wide analysis of piRNA/Piwi-occupied promoter regions during serotonin-mediated synaptic plasticity to obtain a more complete picture of the epigenetic landscape during memory. One attractive possibility is that piRNAs are directed only toward inhibitors of plasticity and that, with each repeated training trial (either behavioral training or pulses of serotonin), the promoters of more inhibitory genes are silenced such that, eventually, the cell is maximally primed and excitable, allowing for the strongest associative memories. Finally, future experiments with chromatin IP of RNA polymerase and/or of Piwi at the CREB2 locus would greatly increase our understanding of the mechanisms governing Piwi-dependent methylation. It would substantiate the idea that Piwi is recruited to CREB2 in an activity-dependent manner and, further, that methylation of the promoter is directly responsible for the observed reduction in transcription of the gene. It is also possible that other small RNAs play a role in epigenetic regulation during plasticity. Irrespective of their biogenesis properties, small RNAs confer versatile sequence specificity to mechanisms of gene regulation, and therefore, any small RNA that evolves functionality for its guide protein to recruit methylation elements to the target promoter could prove equally effective. It is possible, therefore, that one of the many rapidly multiplying classes of nuclear small RNAs takes over the same task in other species.

In summary, we find that Piwi/piRNAs control the activity-dependent epigenetic regulation of the transcription factor CREB2, which may prove to be an important and general mechanism of small RNA-mediated long-lasting regulation of gene expression in neurons that contributes to long-term memory storage. This initial study compels the further exploration of a genome-wide approach toward understanding the extent of small RNA-mediated epigenetic regulation in neurons during learning and memory.

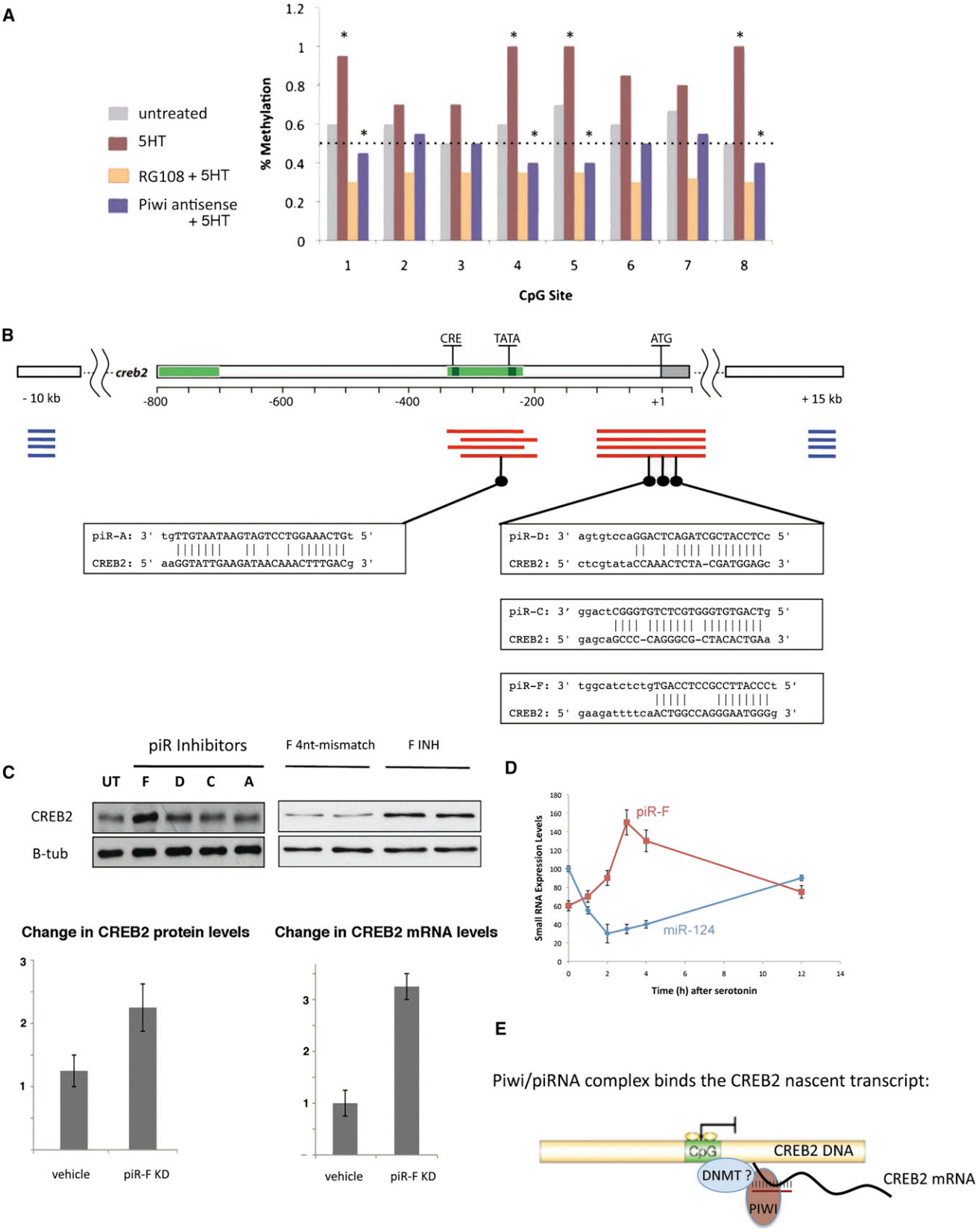
A
untreated
5HT
RG108 + 5HT
Piwi antisense + 5HT
% Methylation
CpG Site
B
creb2
CRE
TATA
ATG
- 10 kb
+ 15 kb
piR-A: 3' tgTTGTAATAAGTAGTCCTGGAAACTGt 5'
CREB2: 5' aaGGTATTGAAGATAACAAACTTTGACg 3'
piR-D: 3' agtgtccaGGACTCAGATCGCTACCTCc 5'
CREB2: 5' ctcgtataCCAAACTCTA-CGATGGAGc 3'
piR-C: 3' ggactCGGGTGTCTCGTGGGTGTGACTg 5'
CREB2: 5' gagcaGCCC-CAGGGCG-CTACACTGAa 3'
piR-F: 3' tggcatctctgTGACCTCCGCCTTACCCt 5'
CREB2: 5' gaagattttcaACTGGCCAGGGAATGGGg 3'
C
piR Inhibitors
F 4nt-mismatch
F INH
UT
F
D
C
A
CREB2
B-tub
Change in CREB2 protein levels
vehicle
piR-F KD
Change in CREB2 mRNA levels
vehicle
piR-F KD
D
piR-F
miR-124
Small RNA Expression Levels
Time (h) after serotonin
E
Piwi/piRNA complex binds the CREB2 nascent transcript:
CpG
CREB2 DNA
DNMT ?
PIWI
CREB2 mRNA

EXPERIMENTAL PROCEDURES

Small RNA Cloning, Sequencing, and Annotation

Tissue preparation and RNA isolation were as described in Rajasethupathy et al. (2009). Starting amount of total RNA was 5 μg per library. Small RNA cloning was performed as described in Hafner et al. (2008), with the exception of using barcoded libraries and the Illumina platform for sequencing. A total of about 15,000 reads was obtained for each solexa library. miRNAs were annotated as described in Rajasethupathy et al., 2009. piRNA candidates were chosen based on their length (between 26 and 33 nt), a 5′ terminal U, and their property of clustering together in a genomic contig (genomic contigs that contained at least 10,000 total piRNA reads, with at least a 60% U start bias, and no more than 1,000 bp interval between individual piRNAs were defined as piRNA clusters); 372 such piRNA clusters were generated. All small RNA sequences were mapped to these clusters, and any clone that mapped perfectly or within one mismatch to a piRNA cluster was annotated as a piRNA.

Pharmacological Treatment, Northern and Western Blot, and Quantitative PCR Analysis

Inhibition of *Aplysia* DNA methyltransferase (DNMT) was performed by incubating ganglia or cultured cells in RG108 (Sigma) at a final concentration of 200 μM. Inhibition of Piwi and piRNAs was carried out using penetratin-conjugated 2′-O-methyl antisense oligoribonucleotides as described in Rajasethupathy et al. (2009). 150 μl of 200 nM penetratin-conjugated oligonucleotides was applied to desheathed pleural ganglia in Eppendorf tubes for a minimum of 8 hr (for piRNA knockdown) and a minimum of 1 day (for Piwi knockdown) before washout, after which RNA or protein was harvested. Northern blot (Landgraf et al., 2007), western blot, and quantitative PCR (Rajasethupathy et al., 2009) were performed as previously described. Probe sequences and antibody information are provided in the Supplemental Information.

Periodate Treatment and Beta Elimination

Total RNA from each *Aplysia* CNS was extracted, ethanol precipitated, and redissolved in 13.5 μl of H_20. 4 μl of borate buffer 1 (25 ml 0.8 M boric acid + 8.75 ml 0.2 M sodiumborate in 100 ml H_2O [pH 8.6]) and 2.5 μl of 0.2 M sodiumperiodate were added to the RNA solution and incubated in the dark at 24°C for 10 min. 5 μl of 50% (v/v) glycerol was added to quench the reaction, and the resulting solution was concentrated in a speedvac to 5 μl. 50 μl of borate buffer 2 (6.25 ml 0.8 M boric acid + 16.875 ml 0.2 M sodiumborate in 400 ml H_2O [pH 9.5] with NaOH) was added and incubated for 90 min at 45°C. RNA was then precipitated in three volumes of ethanol, washed once in 70% ethanol, and run on a 20% acrylamide gel along with untreated total RNA from *Aplysia* CNS, as well as with synthetic piRNA that was either 2′-O-methyl modified at its 3′ end or unmodified, and each was treated or untreated as positive and negative controls, loaded at 30 fmol each with carrier tRNA. Blots were probed for piR-1 and miR-22.

Nuclear/Cytoplasmic Fractionation

Aplysia CNS and heart tissue were subject to nuclear and cytoplasmic extraction using the Pierce NE-PER (Thermo Scientific 78833) kit. All procedures were performed as described in the instruction manual, though we quadrupled all starting volumes so that we may split the extraction in half twice to end up with the following four samples for any given tissue: (1) total RNA, (2) fractioned RNA, (3) total protein, and (4) fractioned protein). For step 6, we redissolved the nuclear pellet in a final volume that would match the cytoplasmic extract, rather than the amount stated in the manual, to allow comparison across fractions and with the total input. The effectiveness of fractionation was confirmed by western blotting the protein fractions and probing for nuclear (histone H3) and cytoplasmic (GAPDH) specific markers. This kit was already optimized for extraction of *Aplysia* CNS and heart tissue but requires further optimization of reagent volumes and incubation times to successfully separate muscle or ovotestes fractions.

DNA Methylation Assays

DNA purification (DNA mini kit; QIAGEN) was performed on *Aplysia* sensory neuron clusters. Purified DNA was then processed for bisulfite modification (Epitect Bisulfite Kit; QIAGEN). Quantitative PCR was used to determine the DNA methylation status of the CREB2 and CREB1 genes. Methylation-specific PCR primers were designed using the Methprimer software (available at http://www.urogene.org/methprimer/). For quantitative methylation analysis through real-time PCR and pyrosequencing of the CREB2, CREB1, and PKA-R promoters, we used the Sequenom massArray facility at Cornell (http://vivo.cornell.edu/display/SequenomMassARRAY), and all primers were designed using the epidesigner software (available at http://www.epidesigner.com/). All primer sequences are provided in the Supplemental Information.

Cell Culture, Injections, Treatments, and Electrophysiology

Cocultures of synaptically paired sensory and motor neurons were prepared as previously reported (Montarolo et al., 1986). For intracellular injections, either a Piwi antisense oligoribonucleotide (5 uM) was used for knockdown of Piwi or a Piwi-GFP expression vector (1 μg/ul) was used for overexpression of Piwi. To generate the pNEX-apPiwi-eGFP, the apPiwi ORF was PCR amplified from cDNA and subcloned into a pNEX3-eGFP vector (Kaang, 1996) modified by the insertion of a Gateway Destination cassette (Invitrogen) within the polylinker (pNEX3-eGFP-DEST vector).

SUPPLEMENTAL INFORMATION

Supplemental Information includes Extended Experimental Procedures and three tables and can be found with this article online at doi:10.1016/j.cell.2012.02.057.

ACKNOWLEDGMENTS

We would like to thank Tom Maniatis and Praveen Sethupathy for comments on the manuscript and for helpful discussions throughout. We also thank Ferdinando Fiumara, Doron Betel, Pavankumar Puvulla, and Pierre Trifilieff for experimental advice and discussions and Frank Grasso for gifting invertebrate CNS samples. We thank Vivian Zhu and Edward Konstantinov for

Figure 6. Piwi/piRNA Complexes Control the Methylation State of the CREB2 Promoter

A. Real-time pyrosequencing of the CREB2 promoter region shows increased methylation in response to 5HT (maroon) that is fully reversed when 5HT is applied in the presence of a Piwi inhibitor (blue). The results were quantified as a mean of four independent trials, and SDs were calculated but were so low that they are not shown on the graphs for clarity of the figure.

(B) A diagram of the CREB2 genomic locus. The CpG islands are marked in green, and the translational ATG start site is indicated. All CpG sites shown in (A) are present within the green bar, indicating the proximal promoter, between the CRE and TATA sites. In red are ESTs mapping to this locus. In blue are piRNA clusters being generated upstream and downstream of the CREB2 locus. piRNAs abundantly generated in trans with potential target sites to transcribed regions (ESTs) from this locus are shown.

(C) Inhibition of aca-piR-F caused a significant upregulation of CREB2 protein and RNA levels when compared to untreated cells or those treated with inhibitors of aca-piR-A, -C, or -D or those treated with 4 nt mismatch (F 4nt-mismatch) oligonucleotides antisense to piR-F. Results are quantified and shown as a mean of three independent trails ± SD.

(D) The time course of aca-piR-F after the initial exposure to 5HT (time 0 hr). The previously described time course of aca-miR-124 is shown for comparison.

(E) Because of a putatitive binding site for piR-F at the translation start site of CREB2 and its proximity to the promoter, we speculate that the Piwi/piR-F complex may bind the CREB2 nascent transcript and may recruit methylation factors (such as DNMT) to regulate the CREB2 promoter.

technical assistance with cell cultures. This work is supported by an HHMI grant P50 HG002806, NIH grant P01 GM073047, and NRSA training grant 5F30MH086267.

Received: August 8, 2011
Revised: November 11, 2011
Accepted: February 24, 2012
Published: April 26, 2012

REFERENCES

Aravin, A., Gaidatzis, D., Pfeffer, S., Lagos-Quintana, M., Landgraf, P., Iovino, N., Morris, P., Brownstein, M.J., Kuramochi-Miyagawa, S., Nakano, T., et al. (2006). A novel class of small RNAs bind to MILI protein in mouse testes. Nature *442*, 203–207.

Aravin, A.A., Sachidanandam, R., Girard, A., Fejes-Toth, K., and Hannon, G.J. (2007). Developmentally regulated piRNA clusters implicate MILI in transposon control. Science *316*, 744–747.

Bailey, C.H., Kandel, E.R., and Si, K. (2004). The persistence of long-term memory: a molecular approach to self-sustaining changes in learning-induced synaptic growth. Neuron *44*, 49–57.

Barreto, G., Schäfer, A., Marhold, J., Stach, D., Swaminathan, S.K., Handa, V., Döderlein, G., Maltry, N., Wu, W., Lyko, F., and Niehrs, C. (2007). Gadd45a promotes epigenetic gene activation by repair-mediated DNA demethylation. Nature *445*, 671–675.

Bartsch, D., Ghirardi, M., Skehel, P.A., Karl, K.A., Herder, S.P., Chen, M., Bailey, C.H., and Kandel, E.R. (1995). *Aplysia* CREB2 represses long-term facilitation: relief of repression converts transient facilitation into long-term functional and structural change. Cell *83*, 979–992.

Betel, D., Sheridan, R., Marks, D., and Sander, C. (2007). Computational analysis of mouse piRNA sequence and biogenesis. PLoS Comp. Biol. *3*, e222.

Brennecke, J., Malone, C.D., Aravin, A.A., Sachidanandam, R., Stark, A., and Hannon, G.J. (2008). An epigenetic role for maternally inherited piRNAs in transposon silencing. Science *322*, 1387–1392.

Callinan, P.A., and Feinberg, A.P. (2006). The emerging science of epigenomics. Hum. Mol. Genet. *15*(Spec No 1), R95–R101.

Crick, F. (1984). Memory and molecular turnover. Nature *312*, 101.

Davis, H.P., and Squire, L.R. (1984). Protein synthesis and memory: a review. Psychol. Bull. *96*, 518–559.

Feng, J., Zhou, Y., Campbell, S.L., Le, T., Li, E., Sweatt, J.D., Silva, A.J., and Fan, G. (2010). Dnmt1 and Dnmt3a maintain DNA methylation and regulate synaptic function in adult forebrain neurons. Nat. Neurosci. *13*, 423–430.

Fiore, R., Khudayberdiev, S., Christensen, M., Siegel, G., Flavell, S.W., Kim, T.K., Greenberg, M.E., and Schratt, G. (2009). Mef2-mediated transcription of the miR379-410 cluster regulates activity-dependent dendritogenesis by fine-tuning Pumilio2 protein levels. EMBO J. *28*, 697–710.

Girard, A., Sachidanandam, R., Hannon, G.J., and Carmell, M.A. (2006). A germline-specific class of small RNAs binds mammalian Piwi proteins. Nature *442*, 199–202.

Grivna, S.T., Beyret, E., Wang, Z., and Lin, H. (2006). A novel class of small RNAs in mouse spermatogenic cells. Genes Dev. *20*, 1709–1714.

Guan, Z., Giustetto, M., Lomvardas, S., Kim, J.H., Miniaci, M.C., Schwartz, J.H., Thanos, D., and Kandel, E.R. (2002). Integration of long-term-memory-related synaptic plasticity involves bidirectional regulation of gene expression and chromatine structure. Cell *111*, 483–493.

Guang, S., Bochner, A.F., Burkhart, K.B., Burton, N., Pavelec, D.M., and Kennedy, S. (2010). Small regulatory RNAs inhibit RNA polymerase II during the elongation phase of transcription. Nature *465*, 1097–1101.

Han, J.H., Kushner, S.A., Yiu, A.P., Cole, C.J., Matynia, A., Brown, R.A., Neve, R.L., Guzowski, J.F., Silva, A.J., and Josselyn, S.A. (2007). Neuronal competition and selection during memory formation. Science *316*, 457–460.

Hayer, A., and Bhalla, U.S. (2005). Molecular switches at the synapse emerge from receptor and kinase traffic. PLoS Comput. Biol. *1*, 137–154.

Hobert, O. (2008). Gene regulation by transcription factors and microRNAs. Science *319*, 1785–1786.

Kirino, Y., and Mourelatos, Z. (2007). Mouse Piwi-interacting RNAs are 2′-O-methylated at their 3′. Nat. Struct. Mol. Biol. *14*, 347–348.

Krol, J., Loedige, I., and Filipowicz, W. (2010a). The widespread regulation of microRNA biogenesis, function and decay. Nat. Rev. Genet. *11*, 597–610.

Krol, J., Busskamp, V., Markiewicz, I., Stadler, M.B., Ribi, S., Richter, J., Duebel, J., Bicker, S., Fehling, H.J., Schübeler, D., et al. (2010b). Characterizing light-regulated retinal microRNAs reveals rapid turnover as a common property of neuronal microRNAs. Cell *141*, 618–631.

Kuramochi-Miyagawa, S., Watanabe, T., Gotoh, K., Totoki, Y., Toyoda, A., Ikawa, M., Asada, N., Kojima, K., Yamaguchi, Y., Ijiri, T.W., et al. (2008). DNA methylation of retrotransposon genes is regulated by Piwi family members MILI and MIWI2 in murine fetal testes. Genes Dev. *22*, 908–917.

Landgraf, P., Rusu, M., Sheridan, R., Sewer, A., Iovino, N., Aravin, A., Pfeffer, S., Rice, A., Kamphorst, A.O., Landthaler, M., et al. (2007). A mammalian microRNA expression atlas based on small RNA library sequencing. Cell *129*, 1401–1414.

Lee, E.J., Banerjee, S., Zhou, H., Jammalamadaka, A., Arcila, M., Manjunath, B.S., and Kosik, K.S. (2011). Identification of piRNAs in the central nervous system. RNA *17*, 1090–1099.

Lisman, J.E. (1985). A mechanism for memory storage insensitive to molecular turnover: a bistable autophosphorylating kinase. Proc. Natl. Acad. Sci. USA *82*, 3055–3057.

Liu, R.Y., Fioravante, D., Shah, S., and Byrne, J.H. (2008). cAMP response element-binding protein 1 feedback loop is necessary for consolidation of long-term synaptic facilitation in *Aplysia*. J. Neurosci. *28*, 1970–1976.

Ma, D.K., Jang, M.H., Guo, J.U., Kitabatake, Y., Chang, M.L., Pow-Anpongkul, N., Flavell, R.A., Lu, B., Ming, G.L., and Song, H. (2009). Neuronal activity-induced Gadd45b promotes epigenetic DNA demethylation and adult neurogenesis. Science *323*, 1074–1077.

Miller, C.A., Gavin, C.F., White, J.A., Parrish, R.R., Honasoge, A., Yancey, C.R., Rivera, I.M., Rubio, M.D., Rumbaugh, G., and Sweatt, J.D. (2010). Cortical DNA methylation maintains remote memory. Nat. Neurosci. *13*, 664–666.

Montarolo, P.G., Goelet, P., Castellucci, V.F., Morgan, J., Kandel, E.R., and Schacher, S. (1986). A critical period for macromolecular synthesis in long-term heterosynaptic facilitation in Aplysia. Science *234*, 1249–1254.

Moroz, L.L., Edwards, J.R., Puthanveettil, S.V., Kohn, A.B., Ha, T., Heyland, A., Knudsen, B., Sahni, A., Yu, F., Liu, L., et al. (2006). Neuronal transcriptome of *Aplysia*: neuronal compartments and circuitry. Cell *127*, 1453–1467.

Price, J.C., Guan, S., Burlingame, A., Prusiner, S.B., and Ghaemmaghami, S. (2010). Analysis of proteome dynamics in the mouse brain. Proc. Natl. Acad. Sci. USA *107*, 14508–14513.

Rai, K., Huggins, I.J., James, S.R., Karpf, A.R., Jones, D.A., and Cairns, B.R. (2008). DNA demethylation in zebrafish involves the coupling of a deaminase, a glycosylase, and gadd45. Cell *135*, 1201–1212.

Rajasethupathy, P., Fiumara, F., Sheridan, R., Betel, D., Puthanveettil, S.V., Russo, J.J., Sander, C., Tuschl, T., and Kandel, E. (2009). Characterization of small RNAs in *Aplysia* reveals a role for miR-124 in constraining synaptic plasticity through CREB. Neuron *63*, 803–817.

Rybak, A., Fuchs, H., Smirnova, L., Brandt, C., Pohl, E.E., Nitsch, R., and Wulczyn, F.G. (2008). A feedback loop comprising lin-28 and let-7 controls pre-let-7 maturation during neural stem-cell commitment. Nat. Cell Biol. *10*, 987–993.

Saito, K., and Siomi, M.C. (2010). Small RNA-mediated quiescence of transposable elements in animals. Dev. Cell *19*, 687–697.

Serrano, P., Friedman, E.L., Kenney, J., Taubenfeld, S.M., Zimmerman, J.M., Hanna, J., Alberini, C., Kelley, A.E., Maren, S., Rudy, J.W., et al. (2008). PKMzeta maintains spatial, instrumental, and classically conditioned long-term memories. PLoS Biol. *6*, 2698–2706.

Si, K., Lindquist, S., and Kandel, E.R. (2003). A neuronal isoform of the *aplysia* CPEB has prion-like properties. Cell *115*, 879–891.

Si, K., Choi, Y.B., White-Grindley, E., Majumdar, A., and Kandel, E.R. (2010). *Aplysia* CPEB can form prion-like multimers in sensory neurons that contribute to long-term facilitation. Cell *140*, 421–435.

Song, H., Smolen, P., Av-Ron, E., Baxter, D.A., and Byrne, J.H. (2007). Dynamics of a minimal model of interlocked positive and negative feedback loops of transcriptional regulation by cAMP-response element binding proteins. Biophys. J. *92*, 3407–3424.

Verdel, A., Jia, S., Gerber, S., Sugiyama, T., Gygi, S., Grewal, S.I., and Moazed, D. (2004). RNAi-mediated targeting of heterochromatin by the RITS complex. Science *303*, 672–676.

Wassenegger, M. (2005). The role of the RNAi machinery in heterochromatin formation. Cell *122*, 13–16.

Watanabe, T., Takeda, A., Tsukiyama, T., Mise, K., Okuno, T., Sasaki, H., Minami, N., and Imai, H. (2006). Identification and characterization of two novel classes of small RNAs in the mouse germline: retrotransposon-derived siRNAs in oocytes and germline small RNAs in testes. Genes Dev. *20*, 1732–1743.

Wayman, G.A., Davare, M., Ando, H., Fortin, D., Varlamova, O., Cheng, H.Y., Marks, D., Obrietan, K., Soderling, T.R., Goodman, R.H., and Impey, S. (2008). An activity-regulated microRNA controls dendritic plasticity by down-regulating p250GAP. Proc. Natl. Acad. Sci. USA *105*, 9093–9098.

Weaver, I.C., Cervoni, N., Champagne, F.A., D'Alessio, A.C., Sharma, S., Seckl, J.R., Dymov, S., Szyf, M., and Meaney, M.J. (2004). Epigenetic programming by maternal behavior. Nat. Neurosci. *7*, 847–854.

Won, J., and Silva, A.J. (2008). Molecular and cellular mechanisms of memory allocation in neuronetworks. Neurobiol. Learn. Mem. *89*, 285–292.

Cell

EXTENDED EXPERIMENTAL PROCEDURES

Sequences Used in This Study

Antisense Sequence Used for Piwi Knockdown

Piwi-AS, GGUCGGGUUGAUCACCACAACUAG.

Antisense Sequences Used for piRNA Knockdowns

piR-A, ACAACATTATTCATCAGGACCTTTGACA; piR-C, CCTGAGCCCACAGAGCACCCACACTGAC; piR-D, TCACAGGTCCTGA GTCTAGCGATGGAGGA; piR-F, ACCGTAGAGACACTGGAGGCGGAATGGGA.

Probe Sequences Used for Northerns

piR-1, AAGCAGAACTTCTCGAGGACCGGATGGA; piR-2, GGCTAGTCCTTGTTGCCCCAATTGCCA; piR-3, CCCATCGTAGATTATG AAGTGCTTACTA; piR-4, GCGAACGTACAAAACATCAGACTCACCA; piR-11, CCACCGTTCGGGCATCGTACTTGGTA; piR-15, TTA CAGCCGGCTCTGGTACATAGACCA; piR-F, ACCGTAGAGACACTGGAGGCGGAATGGGA; miR-22, ACAGCCCTTCATTTGGCA GCTC; tRNA, 5′-TGGAGGGGACACCTGGGTTCGA-3′.

Quantitative Real-Time PCR Primer Sequences

PIWI, GACGATCGCTACTCGGCG; CACCGGAGCTTCCACACAG; CREB2, GCCAGAACATGTCATCATGG; CCTCCCCCTTCTT CTTCATC; CREB1, TCTCGGAAACGGGAATTACG; TTCCCTGGCTGCCTCTCTATT; C/EBP, GCCCCCTACTCCACAAAGTCT; CTGGCCCTCTTATCCACGTACT; GAPDH, GCCTACACCGAGGACGATGT; GGCGGTGTCTCCCTTAAAGTC.

Methylation-Specific PCR Primers

Detection of Unmethylated CREB2

(USP) GTTTTAAATATTTTTGTGTGAATTTATTGAA; ATCAAAACACAATAAAATCAAACACTAATC.

Detection of Methylated CREB2

(MSP) TATTTTCGTGTGAATTTATCGAAAAT; CCGTCCAATAAAAAAACGAAATAACCGT.

Detection of Unmethylated CREB1

(USP) GGTATTAAGGTTTGAAAAGTTTTGTG; CTCAATTAACCTCATAACAATCAAT.

Detection of Methylated CREB

(MSP) GGTATTAAGGTTTGAAAAGTTTTGC; CAATTAACGTCCTAACGATCGAT.

Sequenom Primers

CREB2

aggaagagagAGGTGGTTTATTATTTTTTATGTTTG; cagtaatacgactcactatagggagaaggctCTCCAAAAATCCAACTCCATC.

CREB1

aggaagagagTTGTATATTTTGGATTTATGATAAGTTG; cagtaatacgactcactatagggagaaggctCAAATAACCAAACCATAACTTTAACC.

PKA-R

aggaagagagAAAGTTTTGTTTTTTTGATTGGTTT; cagtaatacgactcactatagggagaaggctACTATTTCACAAATAATTTCTACTCACA.

Antibody Information

The following commercial antibodies were used: CREB1 (New England Biolabs) 1:1000, C/EBP (Cell Signaling, Inc.) 1:3000, Tubulin (Sigma-Aldrich) 1:10000, Ago (Abcam, Inc) 1:3000, Piwi (Abcam, Inc.) 1:3000. CREB2, KHC, and CPEB were polyclonal antibodies previously raised in the laboratory. *Aplysia* polyclonal Piwi antibodies were raised for the current project against the following two peptides: NQADWSREATRNELIC and CQAPFRKELVNEKIET. Following incubation with primary antibodies, a 1:10000 dilution of either anti-rabbit or anti-mouse antiserum was used to detect protein bands by chemiluminescence (Amersham Biosciences).